Preprints (www.preprints.org) | NOT PEER-REVIEWED | Posted: 22 May 2018 doi:10.20944/preprints201805.0283.v1

Article

Modified Venturini Modulation Method for Matrix Converter Under Unbalanced Input Voltage Conditions

Neerakorn Jarutus [1] and Yuttana Kumsuwan [2,*]

[1, 2] Department of Electrical Engineering, Faculty of Engineering, Chiang Mai University, Chiang Mai, Thailand
[1] nrk.jrt@gmail.com
* Correspondence: yt@eng.cmu.ac.th; Tel.: +66-5394-4135 ext. 4140

Abstract: Based on Venturini method, it is in favor of the modulation technique for controlling the matrix converter due to only use of the comparison between the duty cycles in time domain and the triangular carrier wave for generating the gating signals and the achievable voltage ratio between fundamental output magnitude and fundamental input magnitude to 0.866. However, even with simple modulation method and achieving maximum fundamental output magnitude, the possible input voltage unbalance conditions accordingly influence on the output performances (more reduction and distortion). Thus, a modified Venturini modulation method is presented in this paper, in order to solve the problems of unbalanced input voltage conditions on the matrix converter performances. The proposed strategy is to satisfy the desirable feature of the duty cycle modulating waves, as generated in the event of normal situation. Up to this approach, it can support either single-phase condition or two-phase condition. Performance of the proposed control strategy was verified by the simulated implementation in the MATLAB/Simulink software with showing good steady-state and dynamic operations.

Keywords: Venturini method; matrix converter; unbalanced voltage conditions; carrier-based pulse width modulation (PWM).

1. Introduction

Direct ac-ac matrix converters were developed by Venturini and Alesina [1, 2], in 1980. According to its unique matrix structure consisted of nine bi-directional switches, as drawn in Figure 1, the attractive expediencies, compared with the indirect matrix converter, are the lack of a large dc-link energy storage element, which therefore leads to compact and lightweight size of package, bidirectional energy-flow ability, a reduction in the voltage stress on individual switches, and also extend lifespan. By reason of its included capabilities of adjustable output magnitude and fundamental frequency, it has been used obviously in alternative and continuous development, in various ac electrical utility applications for any industry, including adjustable speed drives for an ac induction motor [3-5], uninterruptible power supplies along with improved control strategies for enhancing the power quality [6, 7] and grid interfacing converters in the renewable energy conversion system [8, 9].

Regarding the modulation methods of the matrix converter, it is well known that a greatly relevant and powerful method is the Venturini modulation proposed in [1] and that has been frequently employed up to now [10-15]. With this method, which is used as a direct transfer function, it can be flexibly used to provide the variable-frequency and -amplitude fundamental output voltages from fixed-frequency and -amplitude sinusoidal input voltages. This can be

© 2018 by the author(s). Distributed under a Creative Commons CC BY license.

Preprints (www.preprints.org) | NOT PEER-REVIEWED | Posted: 22 May 2018 doi:10.20944/preprints201805.0283.v1

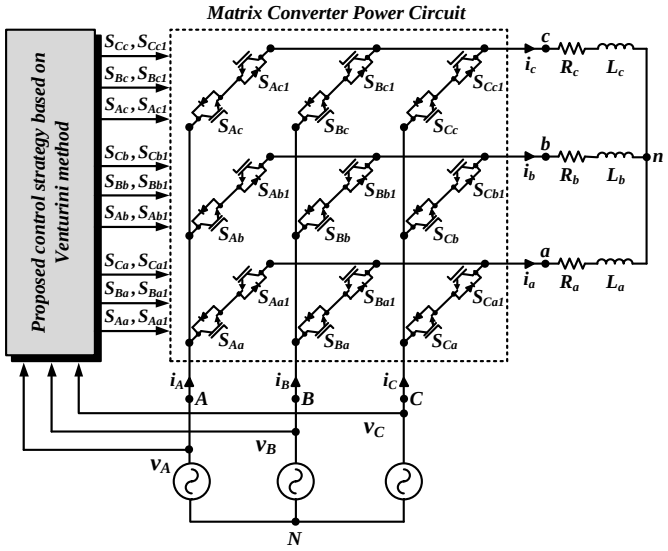

Figure 1. Structure of matrix converter using the proposed modified Venturini modulation method.

achieved a high voltage gain, in terms of output voltage magnitude versus input voltage magnitude, reaching 0.866, which is the maximum gain at this time. In addition, as reported in [16], a low-complexity and good dynamic performances of the Venturini modulation lead to a very convenient modulation method for the matrix converter with the research scope of fixed-frequency output voltage contribution.

One major issue of the matrix converter system is the unbalance of the three-phase input voltage condition, which is a cause of the reduction and/or distortion in the output voltages (and hereby currents). To figure out such a problem, the modified input current modulation strategies, based on the space vector modulation (SVM) algorithm, were proposed in [17-19] to improve the quality of the input currents under unbalanced voltage conditions. However, these strategies are needed the complicated real-timing vector calculations that also depend on all switching operations of the matrix converter. Meanwhile, the feedback compensation strategies via close-loop control, based on the Venturini modulation method were presented in [20, 21]. However, it is difficult to design a feedback system along with elaborate mathematical transfer functions due to the existence of unavoidable non-linear parameters, and also produce the time delay. Another set of the solution is the additional element of the clamp circuit between the input and output sides of the matrix converter, as introduced in [22, 23]. This leads to cumulative hardware component and much more complexity of the control method based on the relevant parasitic component design.

This paper presents a modified Venturini modulation method for the matrix converter under unbalanced input voltage conditions, which is drawn in Figure 1. The salient features of the proposed control strategy are concisely clarified as follows:

- It modifies the modulation strategy based on the Venturini method to regulate constant duty cycle modulating waves despite of having unbalanced input voltage conditions.
- It simplifies the complexity of the analytical mathematic model. That means it does not rely on the implementations of the SVM algorithm and the feedback closed-loop control.
- Any additional hardware element is unnecessary to be installed for solving the effects of the unbalanced input voltages, leading to a low cost solution.

The composition of this paper to support the proposed control strategy is organized as follows. Section 2 briefly discusses the basics of the Venturini modulation method along with its effects under the unbalanced input voltages. The theory of the proposed control strategy to solve the problem is subsequently described in Section 3. Simulation results testifying the proposed control strategy performance are demonstrated in Section 4. Finally, this paper is concluded in Section 5.

Preprints (www.preprints.org) | NOT PEER-REVIEWED | Posted: 22 May 2018 doi:10.20944/preprints201805.0283.v1

2. Overview of Venturini Method

2.1. Structure and Switching Operation of the Matrix Converter

As shown in Figure 1, the structure of the matrix converter consists of eighteen IGBTs in total, where the switching states of each leg are operated within two basic rules [1, 2] as summarized below:

- No two bidirectional switches are turned on in the same horizontal leg. This leads to a short through in a converter leg.
- All the switches cannot be turned off in the same horizontal leg. This might destroy the switches in a converter leg due to the overvoltage.

On account of these two basic rules, there are 3 switching states that allow to operate in one leg of this converter, as listed in Table 1. With these switching states, the switching states of leg b and leg c are also similar to leg a, but they are shifted by $2\pi/3$ rad and $4\pi/3$ rad, respectively. Hence, the switching modes of the matrix converter in three phases are totaling 27 modes, as clearly shown in Figure 2.

Table 1. Switching States per Leg (Leg a) of the Matrix Converter.

Switching states	Switching for Leg a			Phase output voltage v_a
	S_{Aa}	S_{Ba}	S_{Ca}	
A	On	Off	Off	v_A
B	Off	On	Off	v_B
C	Off	Off	On	v_C

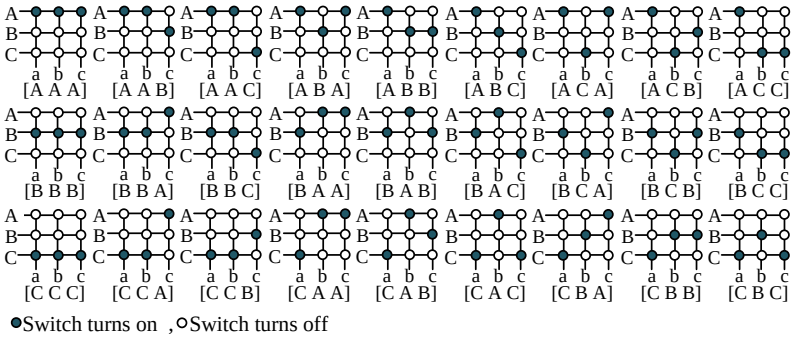

Figure 2. Combination of 27 switching modes of the matrix converter.

From which, the relationship between input voltage ($\mathbf{v}_i(t)$) and output voltage ($\mathbf{v}_o(t)$) can be expressed in the switching function point of view as follow:

$$\mathbf{v}_i(t)=\begin{bmatrix} S_{Aa} & S_{Ba} & S_{Ca} \\ S_{Ab} & S_{Bb} & S_{Cb} \\ S_{Ac} & S_{Bc} & S_{Cc} \end{bmatrix}\mathbf{v}_o(t)\,. \tag{1}$$

Based on (1), it is a further algorithm, which is initially used to find the modulating function in the Venturini modulation method for controlling the matrix converter, as discussed in the next subsection.

2.2. Principle of the Venturini Modulation

Based on the Venturini modulation method, the attainable gating pulse generation for each of the nine bidirectional switches is initially synthesized from the instantaneous three-phase input voltages $(\mathbf{v}_i(t))$, as derived by:

Preprints (www.preprints.org) | NOT PEER-REVIEWED | Posted: 22 May 2018 doi:10.20944/preprints201805.0283.v1

$$\mathbf{v_i}(t)=\begin{bmatrix} v_A \\ v_B \\ v_C \end{bmatrix}=\begin{bmatrix} V_i \sin(\omega_i t) \\ V_i \sin(\omega_i t-2\pi/3) \\ V_i \sin(\omega_i t+2\pi/3) \end{bmatrix}, \quad (2)$$

where V_i denotes the amplitude of the input voltages, $\omega_i = 2\pi f_i$ denotes the fundamental angular frequency of the input voltages. Following (2), it is diagnosed by assuming the condition of the balanced three-phase input voltages.

Taking into consideration this strategy, the output voltages ($\mathbf{v_o}(t)$) related to the input voltages with the direct transfer function can be given as:

$$\mathbf{v_o}(t)=\mathbf{M}(t)\mathbf{v_i}(t), \quad (3)$$

where $\mathbf{M}(t)$ is the transfer matrix of the matrix converter, and also can be defined as:

$$\mathbf{M}(t)=\begin{bmatrix} m_{Aa} & m_{Ba} & m_{Ca} \\ m_{Ab} & m_{Bb} & m_{Cb} \\ m_{Ac} & m_{Bc} & m_{Cc} \end{bmatrix}. \quad (4)$$

Using (4), the transfer matrix consists of the duty cycles for generating the gating pulses of nine bi-directional switches. The comprehensive formula form for all the duty cycles can be accordinglu expressed as:

$$m_{jk}=\frac{1}{3}\left(1+2q_c\frac{v_j v_k}{V_i^2}+\frac{2q}{3q_m}\sin(\omega_j t+\theta_j)\sin(3\omega_j t)\right), \quad (5)$$

where $j=A,B,C$ and $k=a,b,c$. v_j denotes the phase-to-neutral input voltage. v_k denotes the phase-to-neutral output voltage. q denotes the gain of 0.5. q_m denotes the gain of $\sqrt{3}/2 \approx 0.866$. q_c denotes the modulation voltage ratio, which is in the linear modulation range of $0 \le q_c \le 1$.

Analyzing (3) to (5), for a given $q_c = 1$, the maximum magnitude of the fundamental output voltage can be achieved by 0.866 of the input voltage. For extending the technical clarification of the Venturini modulation method, much more detail can be found in [1, 2].

2.3. Statement of Drawbacks

The example under both balanced and unbalanced input voltage conditions with the Venturini modulation method at the modulation voltage ratio q_c of 1 is demonstrated in Figure 3(a), where the specific parameters listed in Table 2 are used. Before 0.2 s, the balanced input voltage condition affects the symmetrical waveforms of pole voltages v_{aN}, v_{bN}, and v_{cN} along with the line-to-line output voltage v_{ab} and currents i_a, i_b, and i_c. Hence, as shown in Figure 4(a) and Figure 5(a), the fundamental output voltage magnitudes approach around 0.866 of input voltages. In the contrary, it can again be observed from Figure 3(a) that when the unbalanced input voltage condition (on phase A) occurred after 0.2 s, the duty cycles in the only first column of (4), i.e., M_{Aa} in this figure, are reduced. This is why the output voltages result in asymmetrical waveforms, as it is evident with the purple dashed-line borders. This consequently leads to further reduction and distortion in the output currents and voltages, as investigated in Figures 4(b) and 5(b), respectively. However, when the proposed control strategy is applied, as shown in Figure 3(b) at 0.2 s, the duty cycle M_{Aa} has obviously increased and is equal to that of the period of the balanced input voltage condition. This leads to the reduction of the problems caused by the unbalanced input voltage condition, as can be seen from the incremental fundamental magnitudes of the output currents and voltages along with the reduced magnitudes of their harmonics in Figures 4(c) and 5(c), respectively.

Preprints (www.preprints.org) | NOT PEER-REVIEWED | Posted: 22 May 2018 doi:10.20944/preprints201805.0283.v1

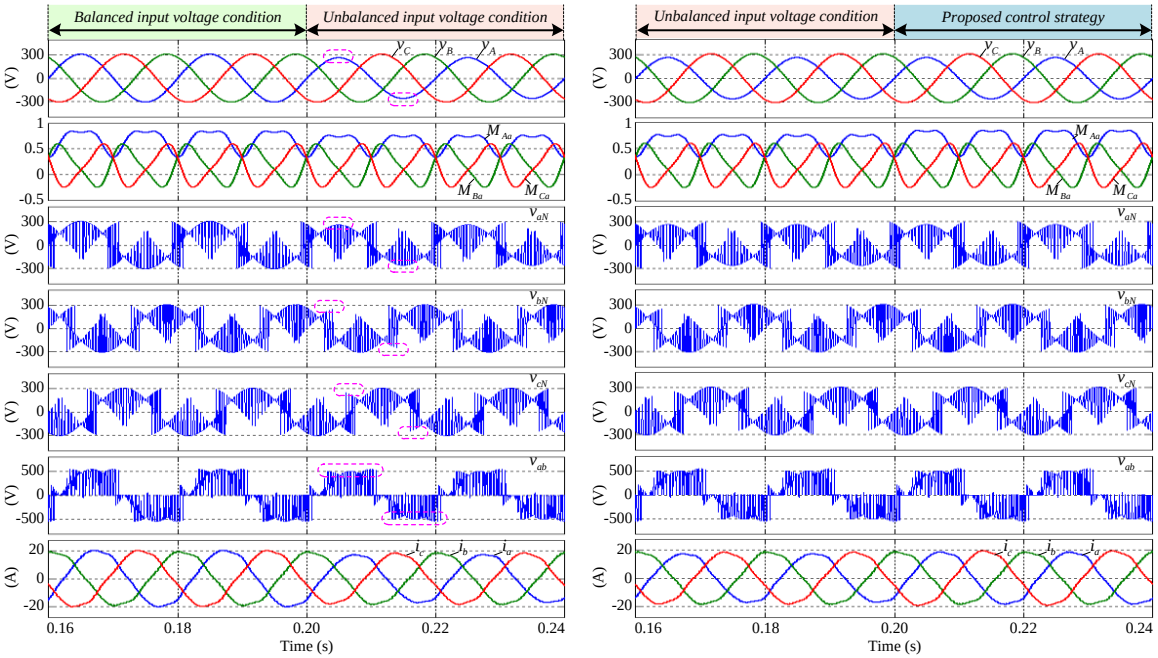

(a) (b)

Figure 3. A transition from (a) balanced input voltage condition to unbalanced input voltage condition with the Venturini method and (b) unbalanced input voltage condition with the Venturini method to unbalanced input voltage condition with the proposed control strategy. (Top to bottom) Waveforms of input voltages v_A, v_B, v_C, duty cycles M_{Aa}, M_{Ba}, M_{Ca}, pole voltages v_{aN}, v_{bN}, v_{cN}, line-to-line output voltage v_{ab}, and output currents i_a, i_b, i_c.

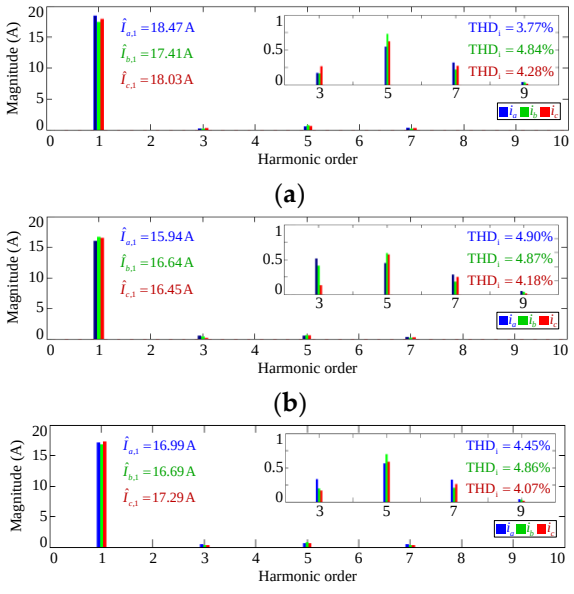

(a) (b) (c)

Figure 4. Harmonic spectrum of output currents for the period of (a) balanced input voltage condition, (b) unbalanced input voltage condition with the Venturini method, and (c) unbalanced input voltage condition with the proposed control strategy.

Preprints (www.preprints.org) | NOT PEER-REVIEWED | Posted: 22 May 2018 doi:10.20944/preprints201805.0283.v1

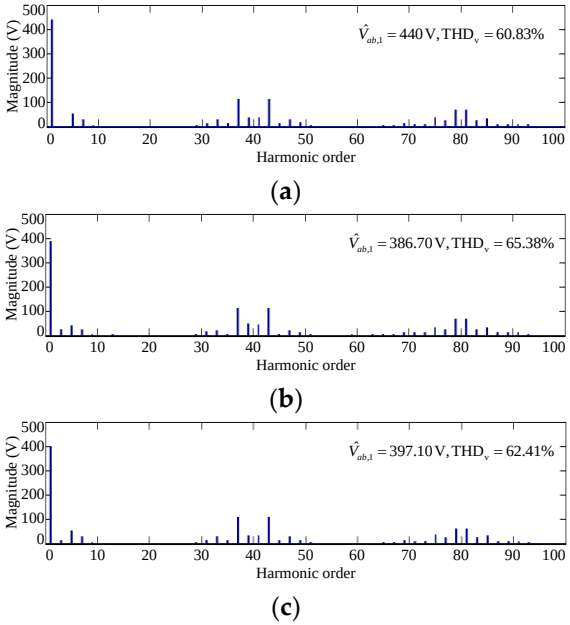

Figure 5. Harmonic spectrum of line-to-line output voltage for the period of (a) balanced input voltage condition, (b) unbalanced input voltage condition with the Venturini method, and (c) unbalanced input voltage condition with the proposed control strategy.

3. Proposed Control Strategy for Matrix Converter

Solving the unbalanced input voltage influences, the use of the proposed control strategy by modifying the modulation of Venturini method in order to regulate the desirable modulation voltage ratio q_c, resulting in keeping the desirable duty cycles to be constant. Based on the duty cycle calculation in (5), to make an analysis with regard to balanced and unbalanced input voltage conditions, the desired reference voltages of the three-phase input voltages are initially given as:

$$v_{j,ref}^{*} = V_{j,ref} \sin\left(\omega_j t + \theta_j\right), \tag{6}$$

where $v_{j,ref}^{*}$ denotes the desired reference voltages of the three-phase input voltages in the normal situation. Subsequent to the check of balanced and unbalanced input voltages, the mean function (v_{mean}) of the three-phase input voltages can be determined as:

$$v_{mean} = \left(v_A + v_B + v_C\right)/3. \tag{7}$$

Considering (7), if the three-phase input voltages are balanced, the mean function v_{mean} becomes 0. Otherwise, it will lead to a tangible appearance. Accordingly, the error (e_j) between the desired input voltage reference and the mean of the three-phase input voltages can be calculated by

$$e_{rj} = v_{j,ref}^{*} - v_{mean}. \tag{8}$$

Using (6) to (8), the proposed modified duty cycle calculation based on the Venturini method can be formulated as

$$M_{jk} = \frac{1}{3}\left(1 + 2q_c \frac{\left(v_{mean} + e_j\right)v_k}{V_i^2} + \frac{2q}{3q_m}\sin\left(\omega_j t + \theta_j\right)\sin\left(3\omega_j t\right)\right). \tag{9}$$

According to (9), the proposed control strategy based on the Venturini method modifies the duty cycle calculation in the terms of the input voltages for regulating it in order to not be varied following the unbalanced input voltages. Later on, these duty cycles are entered into the process of gating pulse generation for driving all the switches of the matrix converter, referring to Figure 6.

Preprints (www.preprints.org) | NOT PEER-REVIEWED | Posted: 22 May 2018 doi:10.20944/preprints201805.0283.v1

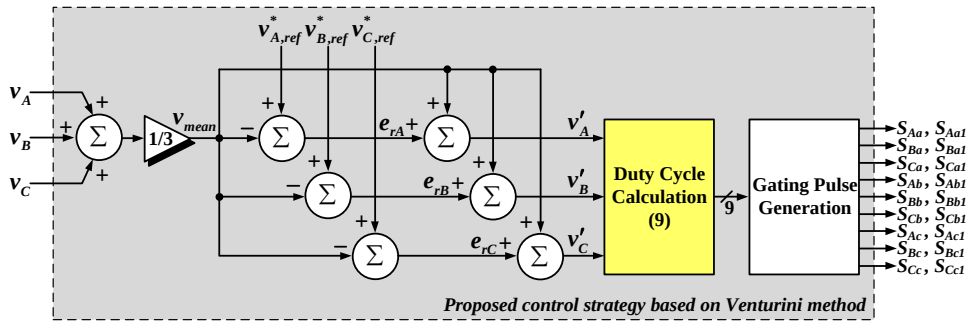

Figure 6. Schematic diagram of the proposed control strategy.

4. Simulation Results

Simulations of the proposed control strategy by modifying the Venturini modulation method for the matrix converter (see Figures 1 and 6) are carried out on the convenient software of MATLAB/Simulink environment in order to verify the theoretical analysis and the proposed control performance. Hereby, the specific parameters indicated in Table 2 are also employed.

Table 2. Parameters Used for Simulation.

Parameters	Symbols	Values	
Three-phase input voltages	v_A, v_B, v_C	220	V
Input frequency	f_s	50	Hz
Output frequency	f_o	50	Hz
Three-phase resistive loads	R_a, R_b, R_c	10	Ω
Three-phase inductive loads	L_a, L_b, L_c	30	mH
Switching frequency	f_{sw}	2	kHz
Modulation voltage ratio	q_c	0.5	

Figure 7 shows the simulated results of the proposed control strategy with the modulation voltage ratio q_c of 0.5 under the 10% step-sag command for single-phase unbalanced input voltage condition on phase A. As shown in Figure 7(a), the mean function v_{mean} results in 0 V for the period of the balanced input voltage condition, as theoretically calculated from (7). Hence, the proposed control algorithm is directly implemented on the Venturini modulation principle. On the contrary, since the phase-A input voltage sags to 280 V, the proposed control strategy is carried out for regulating the duty cycles at q_c of 0.5 with a magnitude of the mean function at 10.33 V. As the results, the patterns of the pole voltages v_{aN}, v_{bN}, and v_{cN} with the proposed control strategy produce the balance and stability for the line-to-line output voltages (v_{ab} for the figure), as well as the three-phase output currents i_a, i_b, and i_c, as directly confirmed by the spectrum of output currents shown in Figure 7(b). The magnitudes of the output voltages can be calculated such that their fundamental components are equivalent to around 50% of the input voltages, which is agreeable and corresponding to theory of the Venturini method.

Similarly, the unbalanced input voltage condition of the 15% step-sag command is demonstrated in Figure 8. With Figure 8(a), the appearance of the mean function v_{mean} in the sag duration resembles that of Figure 7(a), whereas its magnitude further up to around 15.55 V. That means the disturbance of unbalanced input voltages is more intense in comparison to the case of Figure 7. As expected, the duty cycle modulating waves keeping with the constant modulation voltage ratio q_c of 0.5 lead to stable and good qualities of the output voltages and currents. Referring to Figure 8(b), the acceptable harmonic spectrum of output currents is achieved without the reduction in the magnitudes of their fundamental components, including the distortion of the

Preprints (www.preprints.org) | NOT PEER-REVIEWED | Posted: 22 May 2018 doi:10.20944/preprints201805.0283.v1

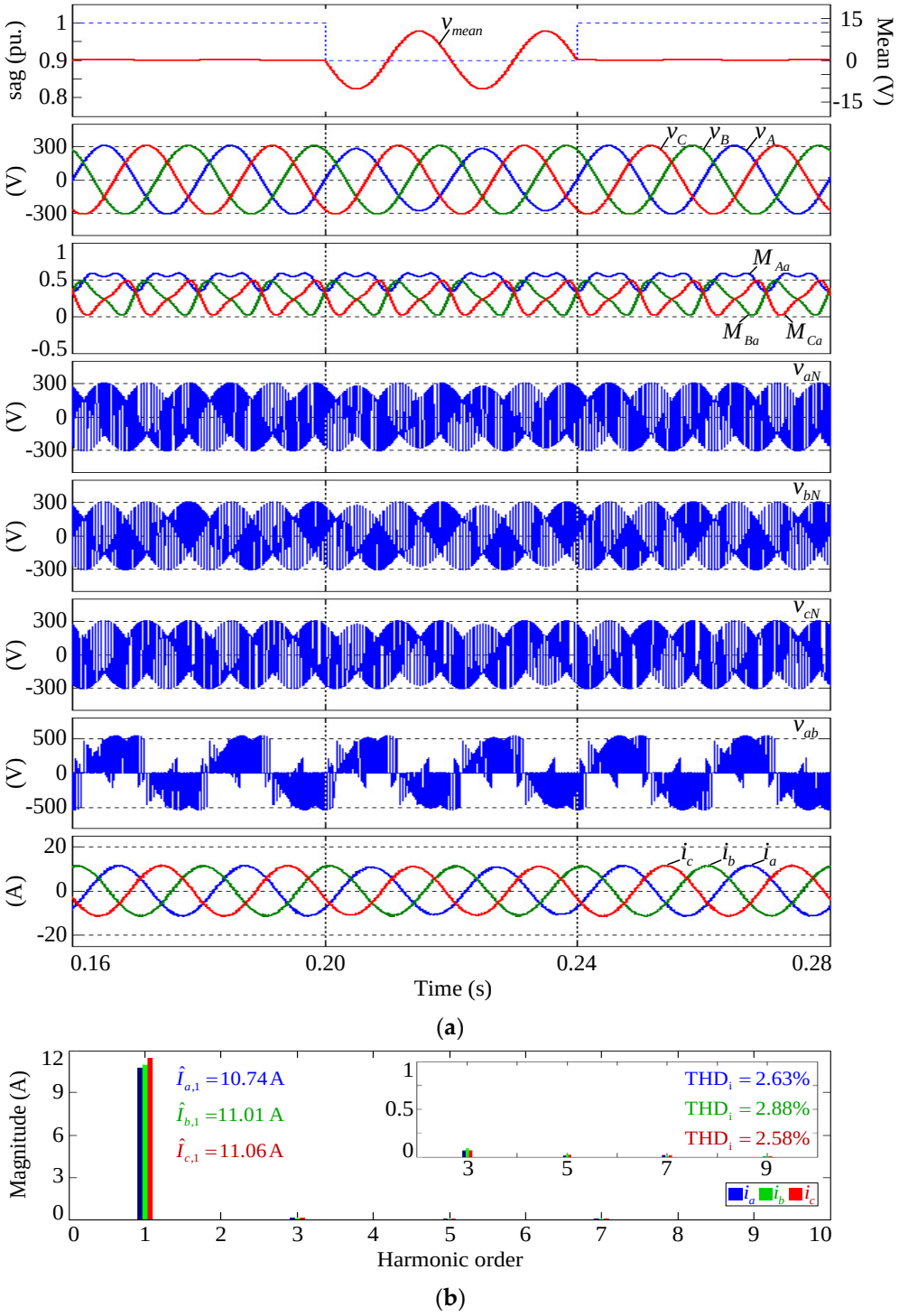

Figure 7. Simulation results with the condition of 10% step-sag single-phase unbalanced input voltage. (a) (Top to bottom) Waveforms of step-sag command and error, three-phase input voltages, duty cycle modulating waves, three-phase pole voltages, line-to-line output voltage, and three-phase output currents. (b) Three-phase output currents harmonic spectrum for unbalanced input voltage duration.

waveforms. This can authenticate the proposed control strategy performance and its theoretical validity.

A set of the simulated results for the 10% step-sag command on phases A and B are shown in Figure 9. Considering 0.2 s to 0.24 s (see Figure 9(a)), owing to the same level of unbalanced input voltage sag, the mean function v_{mean} results in the same magnitude as that of the single-phase unbalanced input voltage condition (see Figure 7(a)), except that its phase angle is led by $90°$.

Preprints (www.preprints.org) | NOT PEER-REVIEWED | Posted: 22 May 2018 doi:10.20944/preprints201805.0283.v1

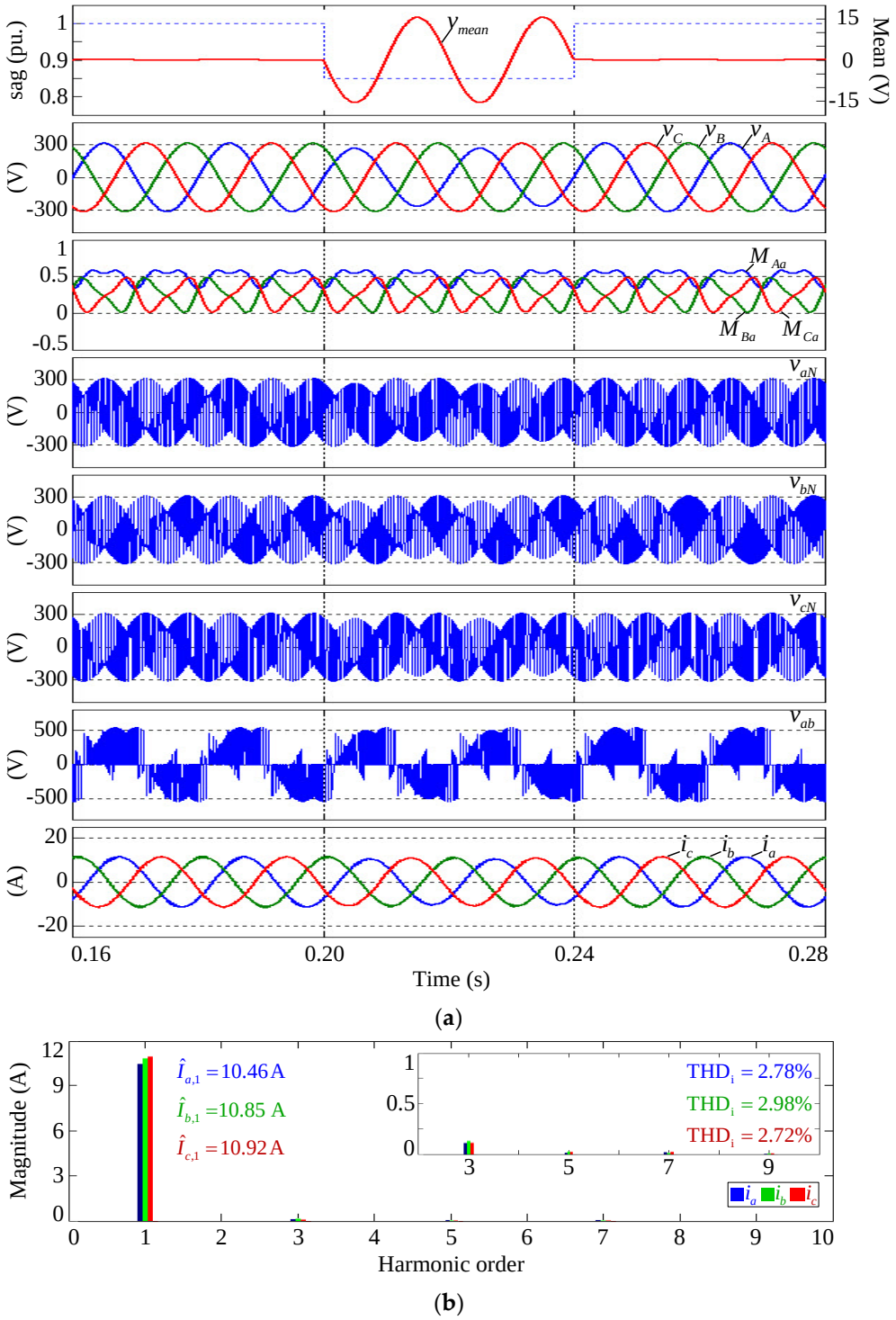

Figure 8. Simulation results with the condition of 15% step-sag single-phase unbalanced input voltage. (a) (Top to bottom) Waveforms of step-sag command and error, three-phase input voltages, duty cycle modulating waves, three-phase pole voltages, line-to-line output voltage, and three-phase output currents. (b) Three-phase output currents harmonic spectrum for unbalanced input voltage duration.

Even though both phase-A and phase-B input voltages unintentionally fall to around 280 V, the output voltages and currents can achieve recognizable qualities and magnitudes for the whole duration. In Figure 9(b), it is evident that the output voltages and currents are still kept a three-phase balanced feature with the performance of the proposed control strategy.

Preprints (www.preprints.org) | NOT PEER-REVIEWED | Posted: 22 May 2018 doi:10.20944/preprints201805.0283.v1

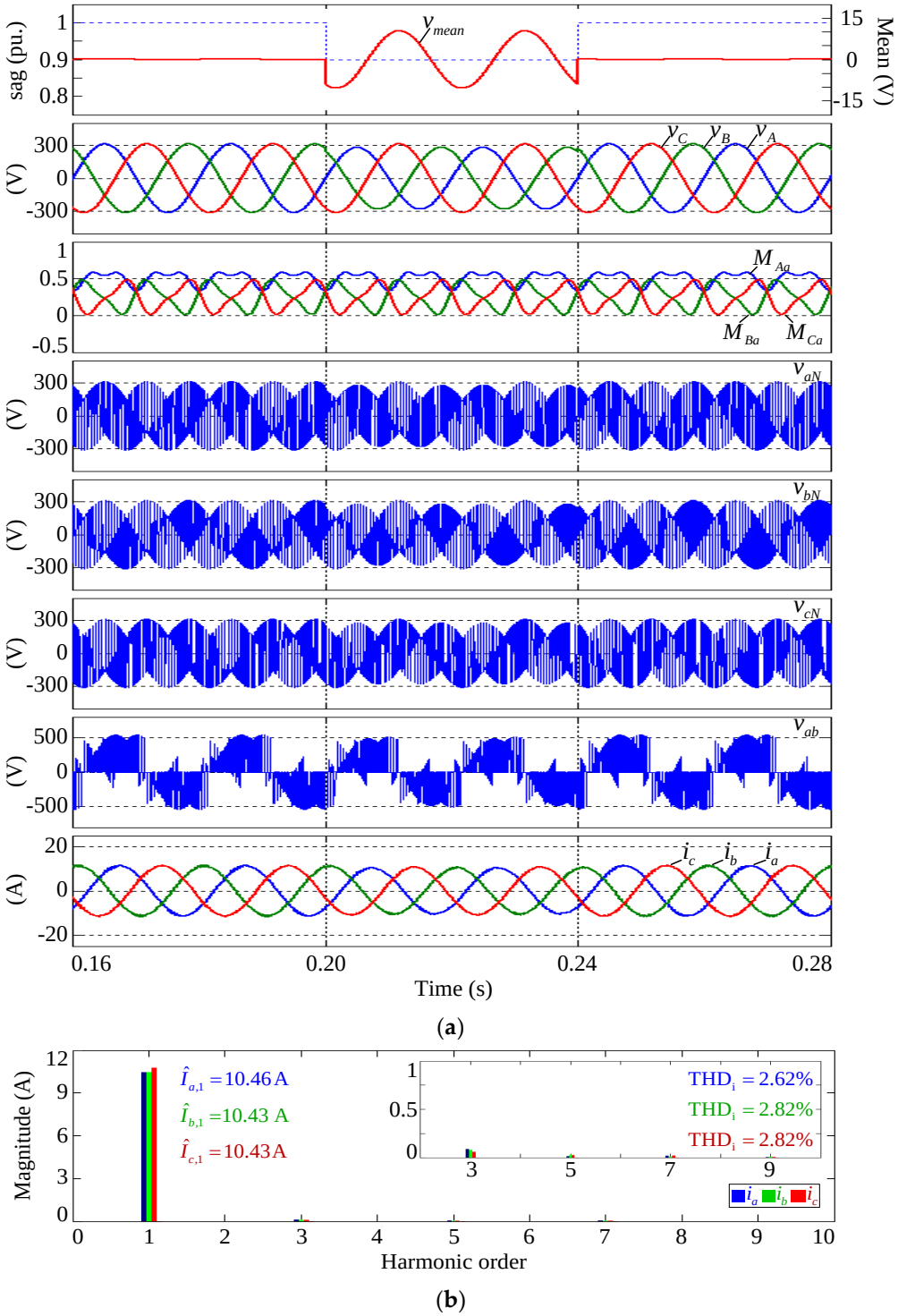

Figure 9. Simulation results with the condition of 10% step-sag two-phase unbalanced input voltages. (a) (Top to bottom) Waveforms of step-sag command and error, three-phase input voltages, duty cycle modulating waves, three-phase pole voltages, line-to-line output voltage, and three-phase output currents. (b) Three-phase output currents harmonic spectrum for unbalanced input voltage duration.

Subsequent to investigation of the proposed control strategy performance under the two-phase unbalanced input voltage condition, the application of the 15% step-sag command on phases A and B is also challenged in Figure 10. As it can be seen in the sag period of the input voltages, the mean function v_{mean} of this case is found to be around 15.55 V (see Figure 10(a)), it has the same magnitude as that of Figure 8(a). A change in the dual-phase (A and B) input voltages does not affect

Preprints (www.preprints.org) | NOT PEER-REVIEWED | Posted: 22 May 2018 doi:10.20944/preprints201805.0283.v1

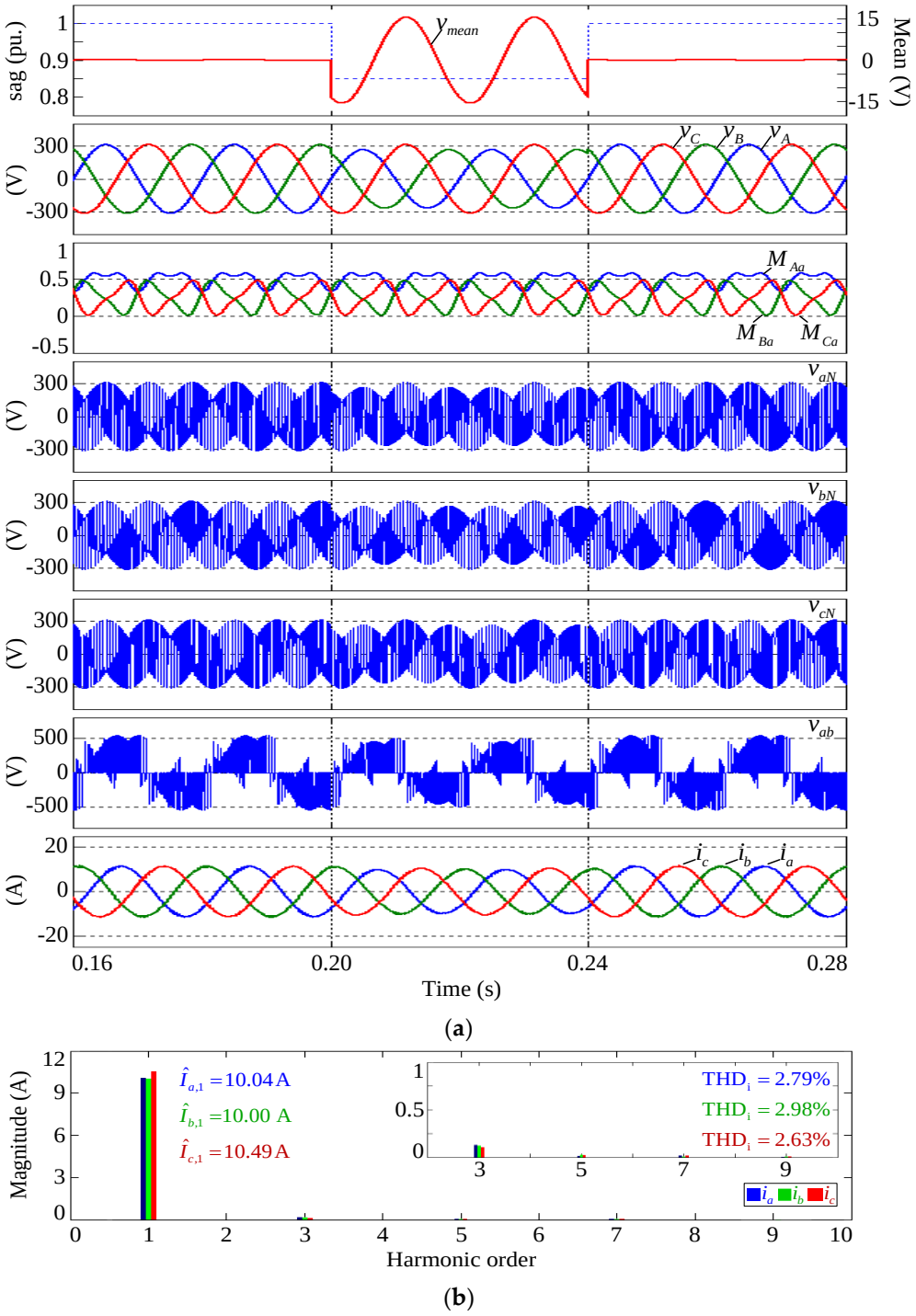

Figure 10. Simulation results with the condition of 15% step-sag two-phase unbalanced input voltages. (a) (Top to bottom) Waveforms of step-sag command and error, three-phase input voltages, duty cycle modulating waves, three-phase pole voltages, line-to-line output voltage, and three-phase output currents. (b) Three-phase output currents harmonic spectrum for unbalanced input voltage duration.

the duty cycles with the proposed control strategy. This is why there are not more distortions in the output voltages and currents, as can be viewed from the corresponding harmonic spectrum in Figure 10(b). For discussion, it is noteworthy that the proposed control strategy is not workable for a case of much more than 15% two-phase unbalanced input voltage condition. That means it is unserviceable for the extreme single-phase and two-phase unbalanced input voltage conditions, including the three-phase unbalanced input voltage conditions.

Preprints (www.preprints.org) | NOT PEER-REVIEWED | Posted: 22 May 2018 doi:10.20944/preprints201805.0283.v1

According to the disagreeable output profiles under 15%-sag unbalanced input voltage condition of the proposed control strategy, as investigated in the previous section, it is consequently evaluated with only 10% sag of single-phase unbalanced input voltage condition. To distinctly confirm the performance of the proposed control strategy, it is also compared with the conventional Venturini method in the point of view of the fundamental output magnitude and the output current quality, as shown in Figures 11(a) and 11(b). The evaluation of Figure 11(a) shows that the proposed control strategy can improve the output magnitude of the matrix converter from the conventional Venturini method under the same conditions as unbalanced input voltages although it produces a lower output magnitude, when compared to that of the normal situation, with a modulation index of greater than 0.5. As the THD_i have been illustrated in Figure 11(b), it is pointed out that the proposed control strategy not only can improve the output magnitude of the matrix converter, but also can develop the output current quality from the conventional Venturini method, when it is operated under unbalanced input voltage condition. Moreover, it also provides the same THD_i tendency, as operated under the non-unbalanced input voltage condition (normal situation). This could confirm the performance of the proposed control strategy for the matrix converter under unbalanced input voltage conditions.

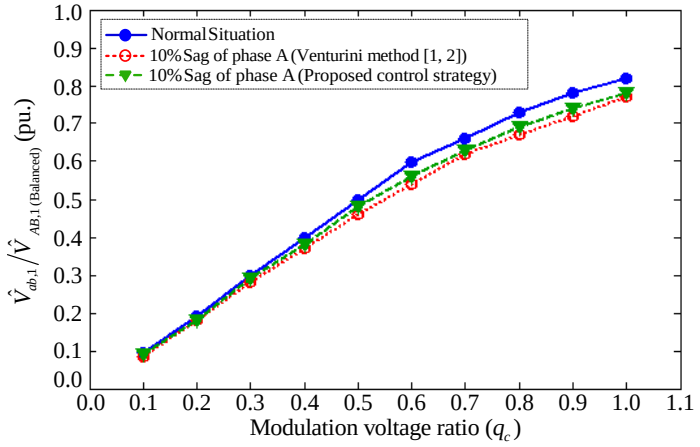

(**a**)

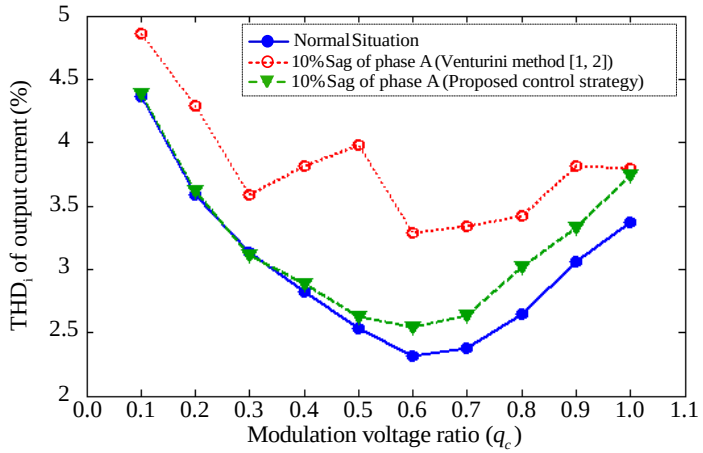

(**b**)

Figure 11. Performance evaluation of the proposed control strategy for the matrix converter compared with the conventional Venturini method ([1, 2]).

5. Conclusion

A control strategy by modifying the Venturini modulation method for matrix converter under unbalanced input voltage conditions is presented in this paper. It is not necessary to consume any additional energy storages, hardware devices, and complicated control algorithms. In the proposed

Preprints (www.preprints.org) | NOT PEER-REVIEWED | Posted: 22 May 2018 doi:10.20944/preprints201805.0283.v1

algorithm, the duty cycle calculation based on the Venturini method is modified by mathematical analyses on the mean function of the measured three-phase input voltages and the error calculations in order to satisfy the desirable stable and balanced output voltages, along with the desirable magnitudes of fundamental components. Among the results, the proposed control strategy is able to eliminate the low-order harmonics of the output voltages and provide as the balanced waveforms under single- and two-phase unbalanced input voltage conditions. Among these reasons, it can also confirm the validity of the theoretical principle and the authenticity of the proposed control strategy performance. Unfortunately, this strategy is unworkable for massive sag voltage conditions of more than 15% and three-phase unbalanced input voltage conditions.

References

1. M. Venturini. A new sine wave in, sine wave out conversion technique which eliminates reactive elements. Seventh National Solid-State Power Conversion Conference, San Diego, California, March 24-27, 1980; pp. E3_1-E3_15.
2. M. Venturini; A. Alesina. The generalised transformer: A new bidirectional sinusoidal waveform frequency converter with continuously adjustable input power factor. IEEE Power Electronics Specialists Conference, Atlanta, Georgia, June 16-20, 1980; pp. 242-252, DOI.
3. P. Nielsen; F. Blaabjerg; J. K. Pedersen. New protection issues of a matrix converter: Design considerations for adjustable-speed drives. IEEE Trans. Ind. Applicat., **1999**, vol. 35, no. 5, pp. 1150-1161, DOI.
4. C. Klumpner; P. Nielsen; I. Boldea; F. Blaabjerg. A new matrix converter motor (MCM) for industry applications. IEEE Trans. Ind. Electron., **2002**, vol. 49, no. 2, pp. 325-335, DOI.
5. D. Orser; N. Mohan. A matrix converter ride-through configuration using input filter capacitors as an energy exchange mechanism. IEEE Trans. Power Electron., **2015**, vol. 30, no. 8, pp. 4377-4385, DOI.
6. H. M. Nguyen; H. Lee; T. Chun. Input power factor compensation algorithms using a new direct-SVM method for matrix converter. IEEE Trans. Ind. Electron., **2011**, vol. 58, no. 1, pp. 232-243, DOI.
7. T. Shi; Y. Yan; H. An; M. Li; C. Xia. Improved double line voltage synthesis strategies of matrix converter for input/output quality enhancement. IEEE Trans. Ind. Electron., **2013**, vol. 60, no. 8, pp. 3034-3046, DOI.
8. H. Hojabri; H. Mokhtari; L. Chang. Reactive power control of permanent-magnet synchronous wind generator with matrix converter. IEEE Trans. Power Del., **2013**, vol. 28, no. 2, pp. 575-584, DOI.
9. S. Monda; D. Kastha. Improved direct torque and reactive power control of a matrix converter-fed grid-connected doubly fed induction generator. IEEE Trans. Ind. Electron., **2015**, vol. 62, no. 12, pp. 7590-7598, DOI.
10. J. Rodriguez; E. Silva; F. Blaabjerg; P. Wheeler; J. Clare; J. Pontt. Matrix converter controlled with the direct transfer function approach: Analysis, modeling and simulation. Int. J. Electron., **2005**, vol. 92, no. 2, pp. 63–85, DOI.
11. P. Wheeler; J. Rodriguez; J. Clare; L. Empringham; A. Weinstein. Matrix converters: A technology review. IEEE Trans. Ind. Electron., **2002**, vol. 49, no. 2, pp. 276–288, DOI.
12. S. Bernet; S. Ponnaluri; R. Teichmann. Design and loss comparison of matrix converters, and voltage-source converters for modern AC drives. IEEE Trans. Ind. Electron., **2002**, vol. 49, no. 2, pp. 304–314, DOI.
13. J. Rzasa. Capacitor clamped multilevel matrix converter controlled with Venturini method. 13th International Power Electronics and Motion Control Conference, Poznan, Poland, September 1-3, 2008; pp. 357–364, DOI.
14. Y. Mei; L. Huang. Improved switching function modulation strategy for three-phase to single-phase matrix converter. IEEE 6th International Power Electronics and Motion Control Conference, Wuhan, China, May 17-20, 2009; pp. 1734–1737, DOI.
15. S. Lopez Arevalo; P. Zanchetta; P. Wheeler; A. Trentin; L. Empringham. Control and implementation of a matrix-converterbased AC-ground power-supply unit for aircraft servicing. IEEE Trans. Ind. Electron., **2010**, vol. 57, no. 6, pp. 2076–2084, DOI.
16. J. Rodriguez; M. Rivera; J. W. Kolar; P. W. Wheeler. A review of control and modulation methods for matrix converters. IEEE Trans. Ind. Electron., **2012**, vol. 59, no. 1, pp. 58-70, DOI.

Preprints (www.preprints.org) | NOT PEER-REVIEWED | Posted: 22 May 2018 doi:10.20944/preprints201805.0283.v1

17. F. Blaabjerg; D. Casadei; C. Klumpner; M. Matteini. Comparison of two current modulation strategies for matrix converters under unbalanced input voltage conditions. IEEE Trans. Ind. Electron., **2002**, vol. 49, no. 2, pp. 289-296, DOI.
18. X. Wang; H. Lin; H. She; B. Feng. A research on space vector modulation strategy for matrix converter under abnormal input-voltage conditions. IEEE Trans. Ind. Electron., **2012**, vol. 59, no. 1, pp. 93-104, DOI.
19. X. Li; M. Su; Y. Sun; H. Dan; W. Xiong. Modulation strategies based on mathematical construction method for matrix converter under unbalanced input voltages. IET Power Electron., **2013**, vol. 6, iss. 3, pp. 434-445, DOI.
20. K. Sun; D. Zhou; L. Huang; K. Matsuse. Compensation control of matrix converter fed induction motor drive under abnormal input voltage conditions. IEEE Industry Applications Conference, Seattle, WA, USA, October 3-7, 2004; pp. 623-630, DOI.
21. H. Karaca; R. Akkaya. Control of Venturini method based matrix converter in input voltage variations. International MultiConference of Engineers and Computer Scientists, Kowloon, Hong Kong, March 18-20, 2009, DOI.